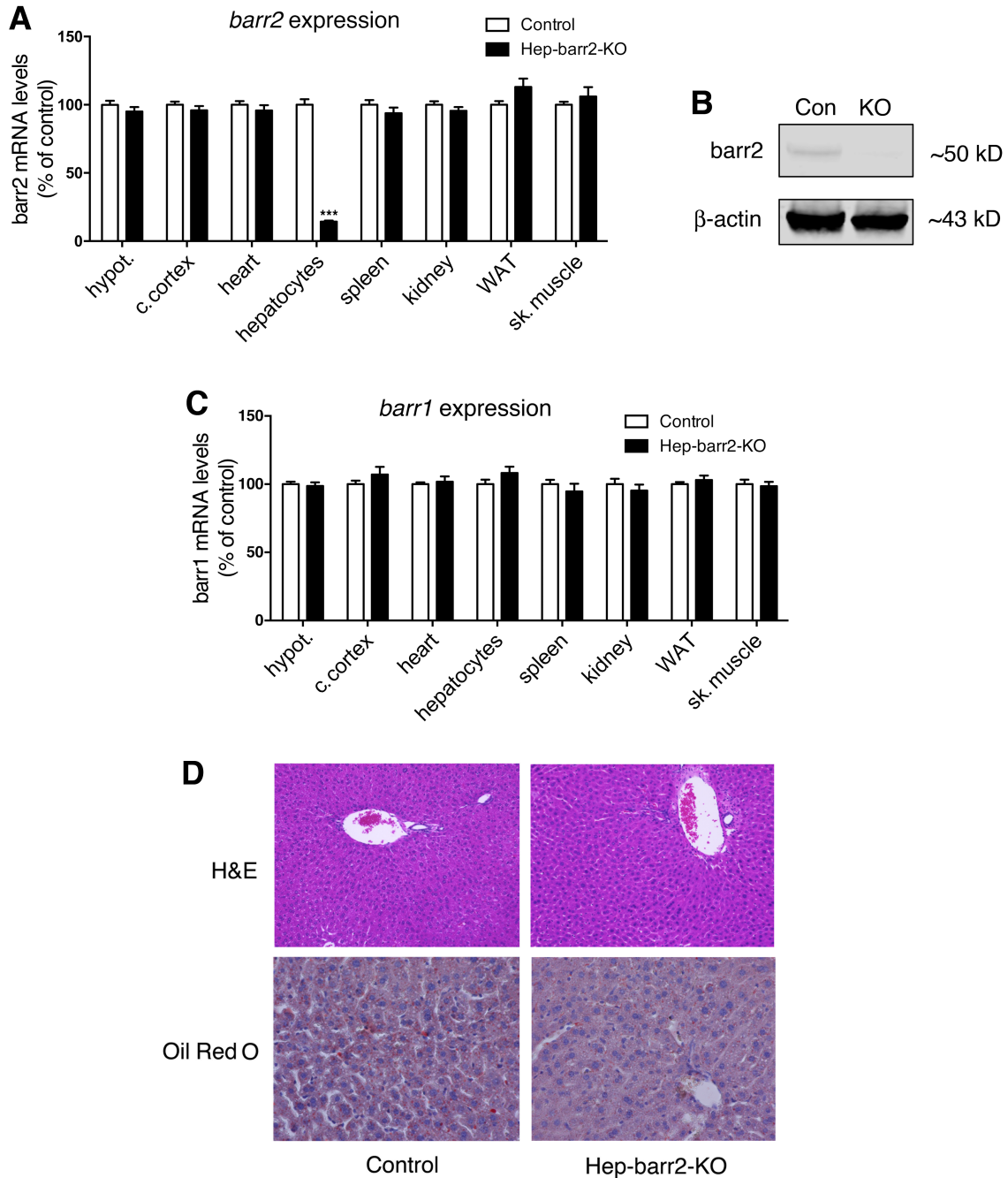


## **Supplemental Data**

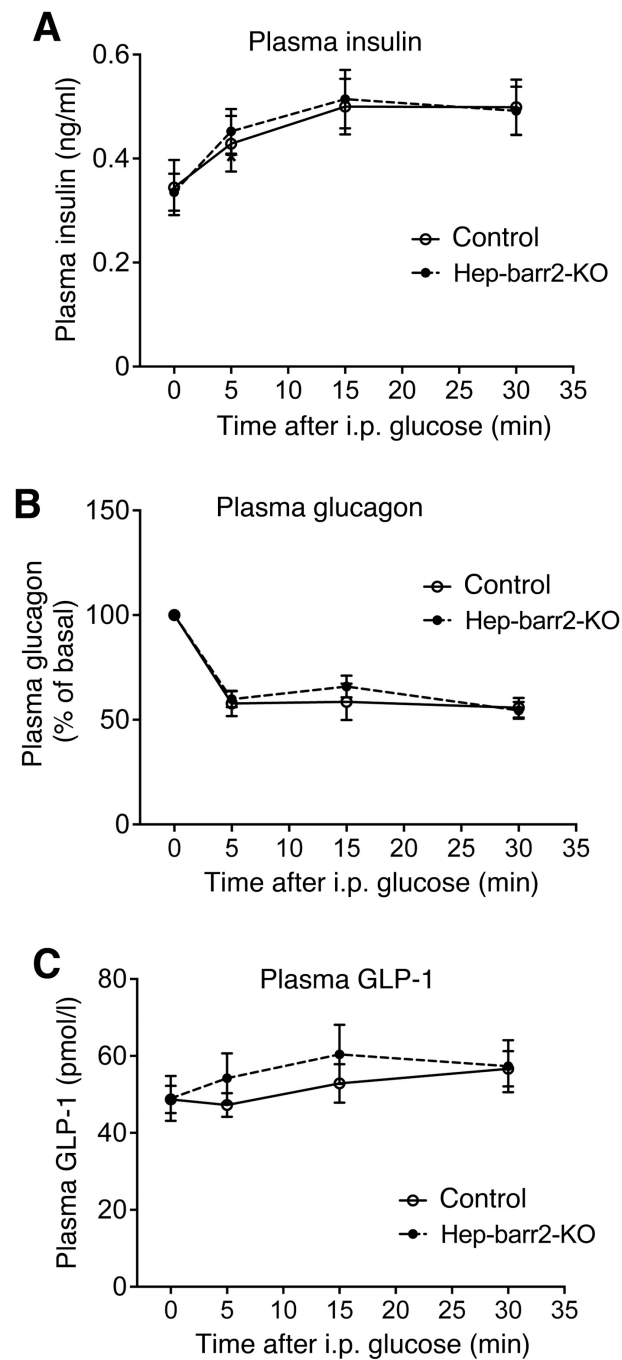
### **Hepatic $\beta$ -arrestin-2 is essential for maintaining euglycemia**

Lu Zhu, Mario Rossi, Yinghong Cui, Regina J. Lee, Wataru Sakamoto, Nicole A. Perry, Nikhil M. Urs, Marc G. Caron, Vsevolod V. Gurevich, Grzegorz Godlewski, George Kunos, Minyong Chen, Wei Chen, and Jürgen Wess

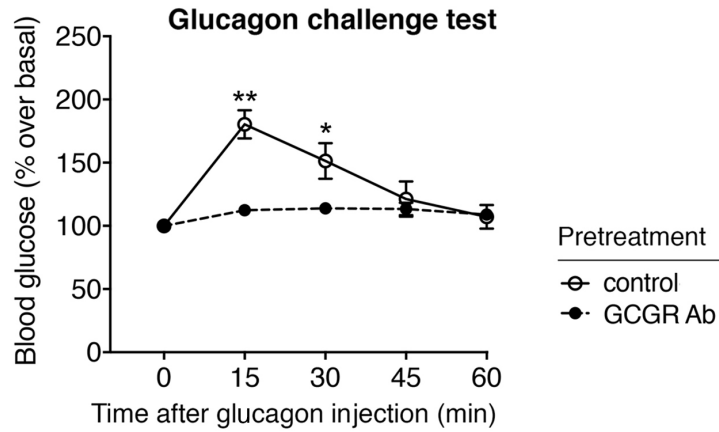


**Supplemental Figure 1. Generation of mutant mice selectively lacking *barr2* in hepatocytes (hep-*barr2*-KO mice) and histochemical studies with liver slices**  
**(A)** *Barr2* transcript levels are selectively reduced in hepatocytes of hep-*barr2*-KO mice.  
**(B)** Representative Western blot indicating the lack of *barr2* protein in hepatocytes of hep-*barr2*-KO mice. The antibody used is selective for *barr2* (Cell Signaling; # 3857).  
**(C)** *Barr1* mRNA levels are not affected by the lack of *barr2* in hepatocytes. *Barr2* and *barr1* transcript levels were examined by qRT-PCR using  $\beta$ -*actin* expression as an internal control. Template RNA was prepared from the indicated tissues. Data are given as means  $\pm$  SEM (3 mice per genotype, 10-week-old males). \*\*\* $p < 0.001$ , as compared to

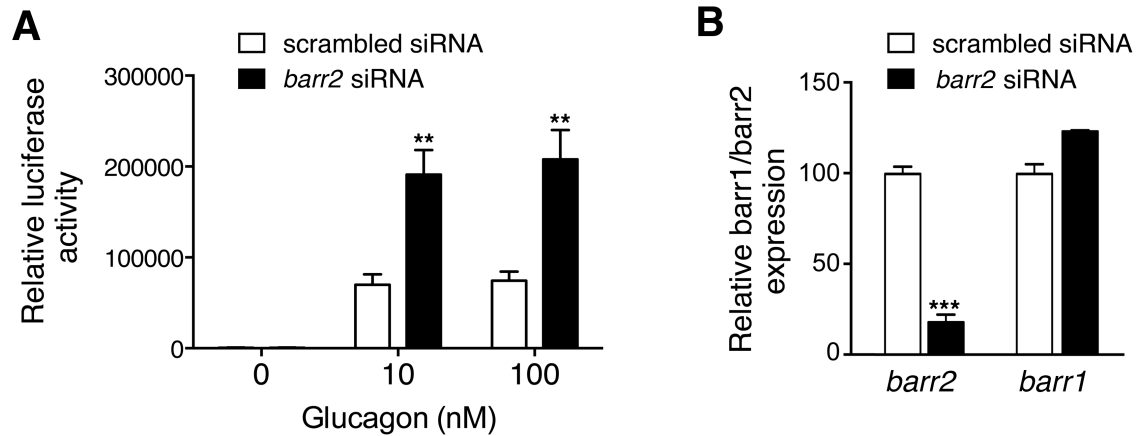
control (Student's t-test). hypoth., hypothalamus; c. cortex, cerebral cortex; WAT, white adipose tissue; sk. muscle, skeletal muscle. **(D)** Lack of barr2 in hepatocytes does not affect mouse liver morphology. Liver sections from fasted hep-barr2-KO mice and their control littermates (10-week-old males) were stained with either H&E (upper panels) or Oil Red O (lower panels). The images shown are representative of results from 10 mice per group.



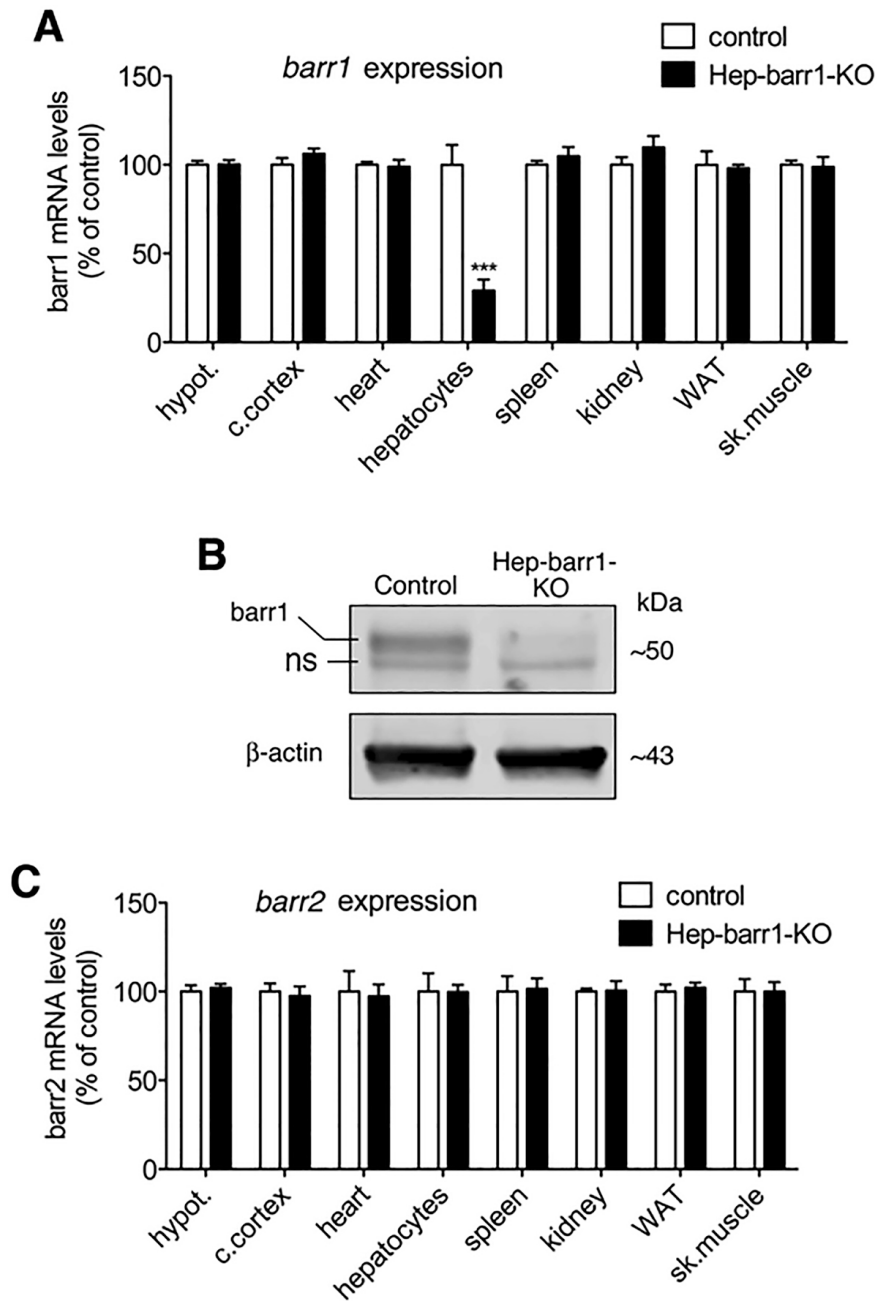
**Supplemental Figure 2. Glucose-induced changes in plasma insulin, glucagon, and GLP-1 remain unaffected by hepatic barr2 deficiency.** (A-C) Hep-barr-2 KO mice and control littermates that had been fasted for 12 hr were injected with glucose (2 g/kg i.p.), followed by the measurement of plasma insulin (A), glucagon (B), and GLP-1 levels (C). Basal glucagon levels at time '0' were (in pmol/l): control,  $3.89 \pm 0.30$ ; hep-barr2-KO,  $3.23 \pm 0.24$ . Data represent means  $\pm$  SEM (n=7 or 8 mice per group; 12-16-week old males).



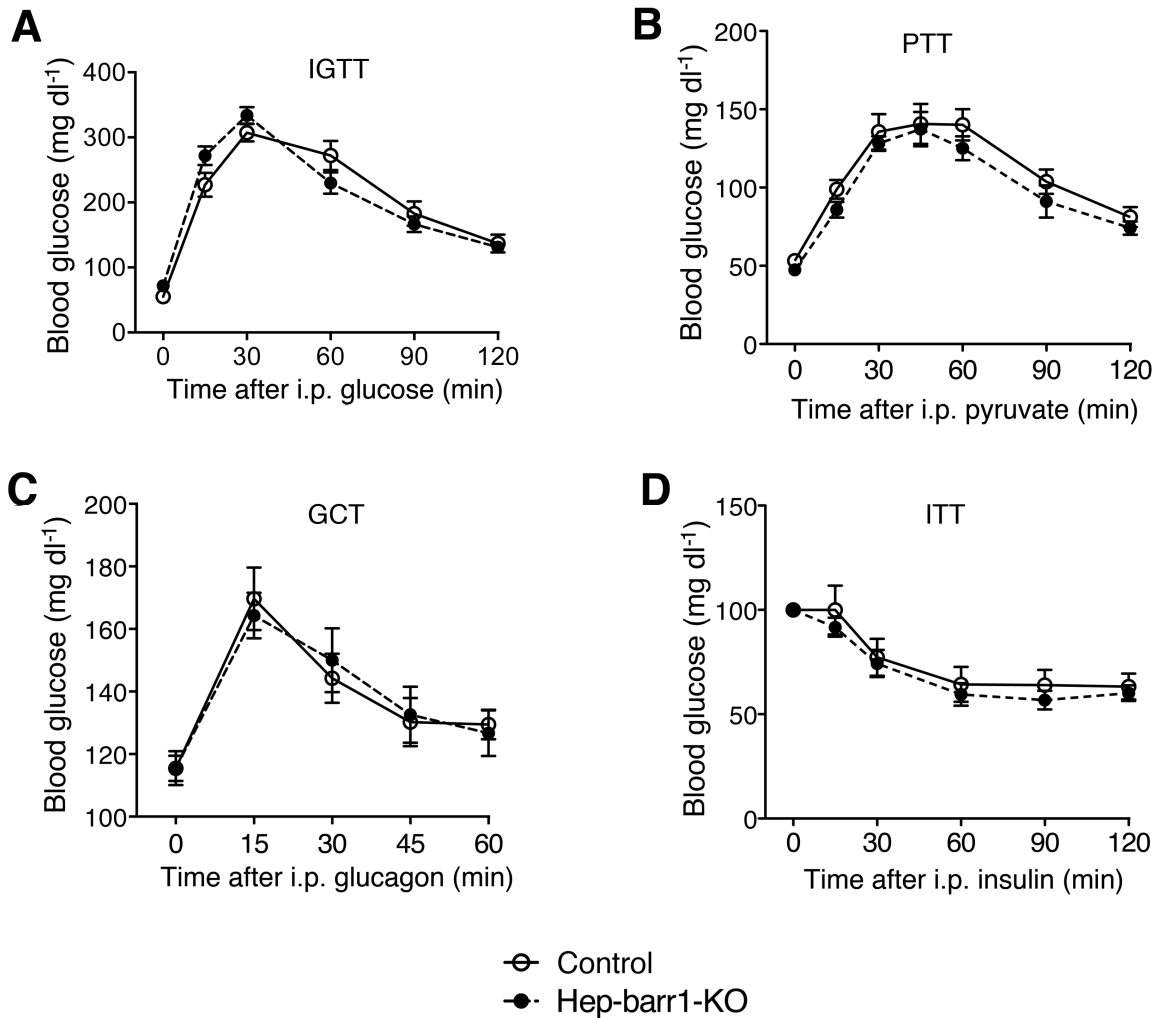
**Supplemental Figure S3. The anti-GCGR antibody blocks glucagon-induced increases in blood glucose levels in WT mice.** Male WT mice (14-week-old male C57BL-6NTac mice) were injected with the anti-GCGR antibody (10 mg/kg i.p.; see Supplemental Methods for details) or vehicle (control) ~24 h prior to glucagon administration (16  $\mu$ g/kg i.p.), following a 4 hr fast. For each individual mouse, blood glucose levels at time '0' were set equal to 100%. Data are given as means  $\pm$  SEM (n=6 per group). \*p<0.05, \*\*p<0.01, versus control (Student's t-test).



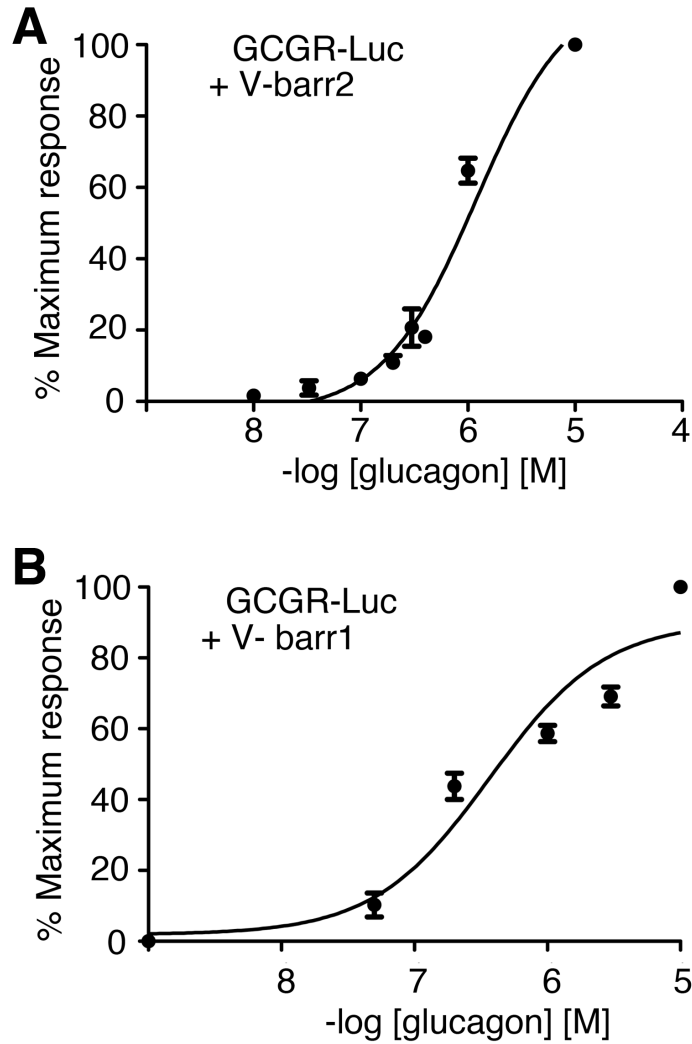
**Supplemental Figure 4. Barr2 knockdown enhances glucagon signaling in primary mouse hepatocytes.** WT mouse hepatocytes were transfected with *barr2* siRNA or scrambled control siRNA. Hepatocytes were then infected with adenoviruses coding for the CRE-luc reporter and  $\beta$ -gal (internal control).  $\beta$ -gal activity was used to normalize the results of luciferases assays. **(A)** Following treatment of hepatocytes with *barr2* siRNA, glucagon enhances cAMP/PKA signaling in a CRE-luc reporter assay. **(B)** Efficient reduction of *barr2* expression after treatment of mouse hepatocytes with *barr2* siRNA. *Barr1* transcript levels were not significantly affected by the knockdown of *barr2* expression. *Barr2* and *barr1* mRNA levels were examined by qRT-PCR using  $\beta$ -actin expression as an internal control. Data are given as means  $\pm$  SEM from six independent experiments. \*\* $p < 0.01$ , \*\*\*  $p < 0.001$ , as compared to control (Student's t-test).



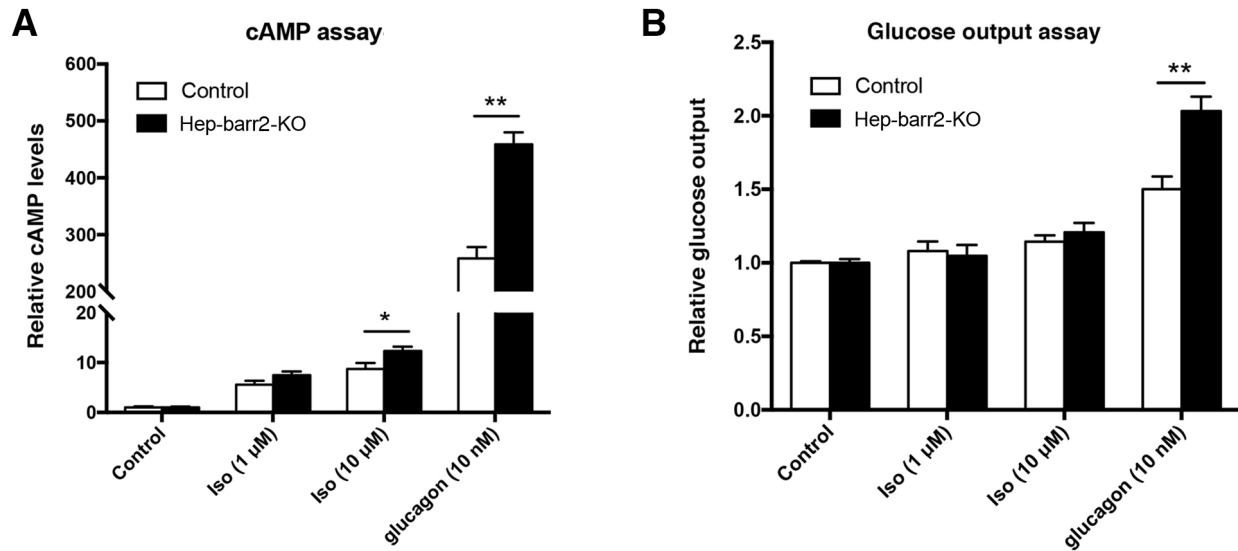
**Supplemental Figure 5. Generation of mutant mice selectively lacking *barr1* in hepatocytes (hep-*barr1*-KO mice).** (A) *Barr1* transcript levels are selectively decreased in hepatocytes of hep-*barr1*-KO mice. (B) Representative Western blot showing the relative lack of *barr1* protein in hepatocytes of hep-*barr1*-KO mice. ns, non-specific band. (C) *Barr2* mRNA levels remain unaffected by hepatocyte *barr1* deficiency. Gene expression levels were determined via qRT-PCR using  $\beta$ -actin expression as an internal control. Template RNA was prepared from the indicated tissues. Data are given as means  $\pm$  SEM (3 mice per genotype, 10-week-old males). \*\*\* $p < 0.001$ , as compared to control (Student's t-test). hypot., hypothalamus; c. cortex, cerebral cortex; WAT, white adipose tissue; sk. muscle, skeletal muscle.



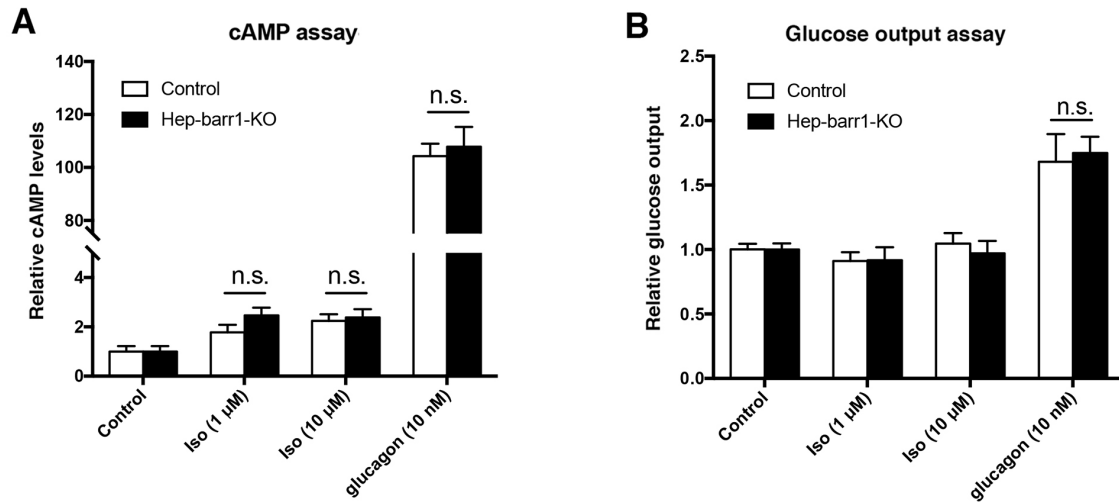
**Supplemental Figure 6. In vivo metabolic studies with hep-barr1-KO mice and their control littermates.** (A) I.p. glucose tolerance test (IGTT). (B) I. p. pyruvate tolerance test (PTT). (C) I.p. glucagon challenge test (GCT). (D) I. p. insulin tolerance test (ITT). All studies were carried out with male mice maintained on regular chow (mouse age: 12-18 weeks). Data are presented as means  $\pm$  SEM (n=7-10 mice per group).



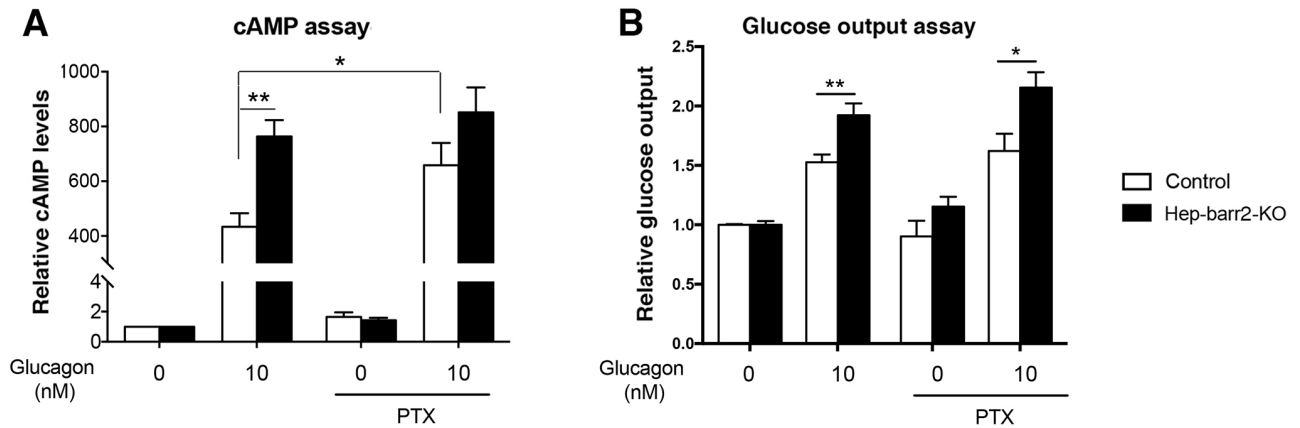
**Supplemental Figure 7. GCGR activation promotes the recruitment of both  $\beta$ -arrestins in BRET assays.** The ability of a GCGR-Luc fusion protein to interact with a Venus-tagged version of barr2 (A) or barr1 (B) was studied using BRET in co-transfected COS-7 cells as a readout (see Supplemental Methods for details). Data represent the means  $\pm$  SEM of three independent experiments.



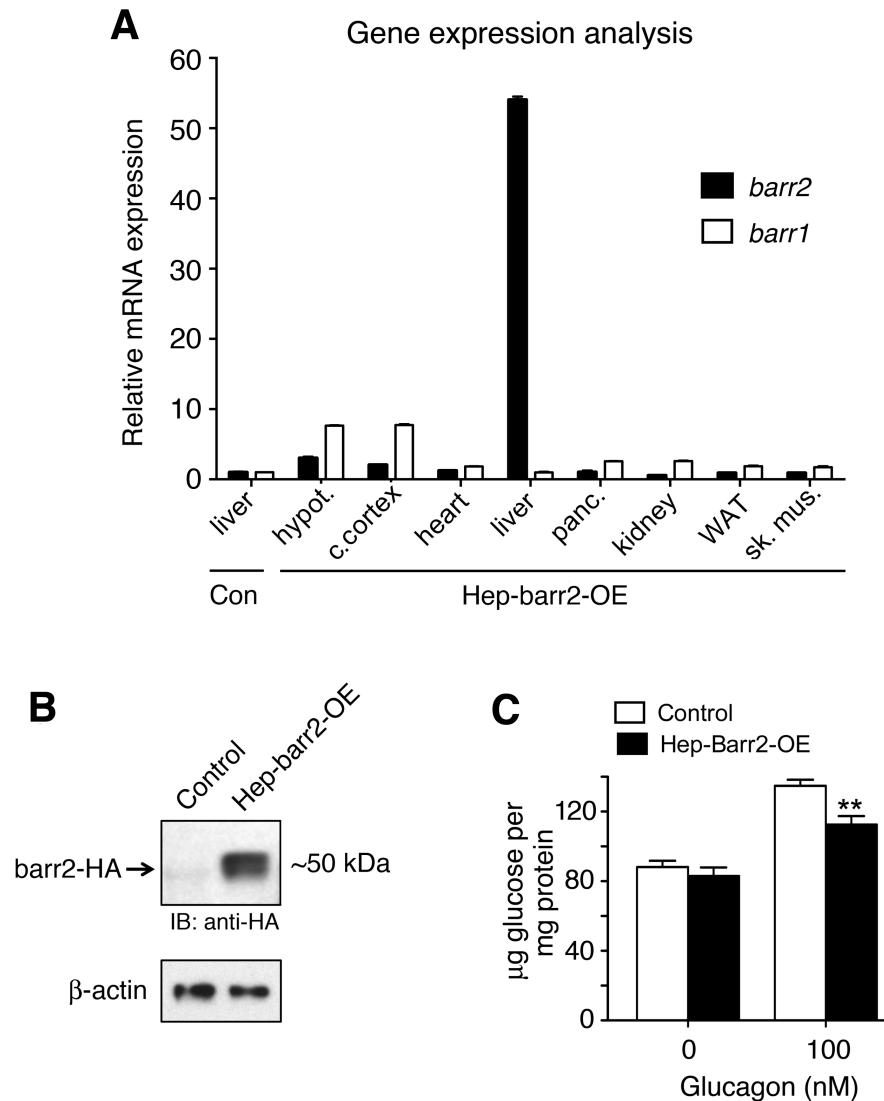
**Supplemental Figure 8. Isoproterenol treatment of primary mouse hepatocytes from control and hep-barr2-KO mice.** (A) cAMP assay. The ability of isoproterenol (Iso), a  $\beta$ -adrenergic receptor agonist, and glucagon to stimulate intracellular cAMP accumulation was examined. In each individual experiment, the cAMP response in the absence of drugs was set equal to 1. (B) Glucose output assay. The ability of Iso and glucagon to stimulate glucose release from control and hep-barr2-KO hepatocytes was determined. In each individual experiment, glucose levels in the absence of drugs were set equal to 1. Data are given as means  $\pm$  SEM of three or four independent experiments. \* $p < 0.05$ , \*\* $p < 0.01$ , versus control (Student's t-test).



**Supplemental Figure 9. Isoproterenol treatment of primary mouse hepatocytes from control and hep-barr1-KO mice. (A) cAMP assay.** The ability of isoproterenol (Iso) and glucagon to stimulate intracellular cAMP production was determined. In each individual experiment, cAMP responses in the absence of drugs were set equal to 1. **(B) Glucose output assay.** The ability of Iso and glucagon to stimulate glucose release from control and hep-barr1-KO hepatocytes was measured. In each individual experiment, glucose levels in the absence of drugs were set equal to 1. Data are given as means  $\pm$  SEM of three independent experiments. n.s., not significantly different from control (Student's t-test).

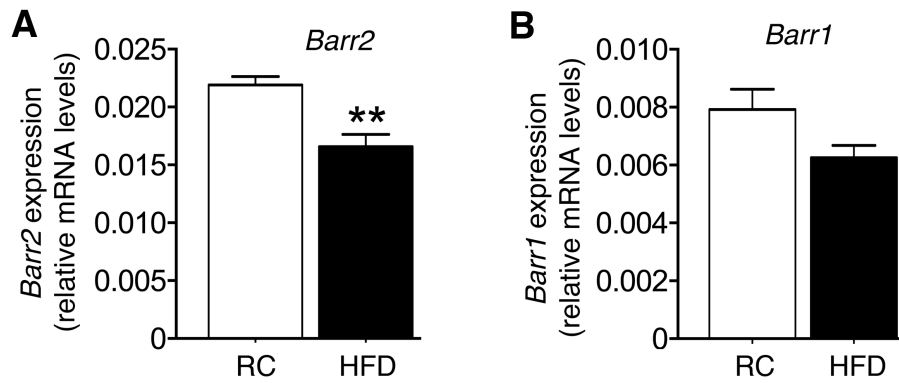


**Supplemental Figure 10. Glucagon treatment of primary mouse hepatocytes from control and hep-barr2-KO mice in the absence or presence of PTX. (A) cAMP assay.** The ability of glucagon to stimulate intracellular cAMP accumulation was examined. In each individual experiment, cAMP responses in the absence of drugs were set equal to 1. **(B) Glucose output assay.** The ability of glucagon to promote glucose release from control and hep-barr2-KO hepatocytes was determined. In each individual experiment, glucose levels in the absence of drugs were set equal to 1. Experiments were carried out either in the absence or presence of PTX (300 ng/ml), including a 2 hr pre-incubation. Data are given as means  $\pm$  SEM of three or four independent experiments. \* $p < 0.05$ , \*\* $p < 0.01$ , versus control (Student's t-test).



**Supplemental Figure 11. Generation of mutant mice selectively overexpressing *barr2* in hepatocytes (hep-barr2-OE mice) and analysis of hepatocyte glucose production.**

(A) *Barr2* transcript levels are selectively increased in the liver of hep-barr2-OE mice. mRNA levels are expressed relative to hepatic *barr2* and *barr1* expression levels in control littermates (=1). *Barr2* and *barr1* transcript levels were examined by qRT-PCR using  $\beta$ -actin expression as an internal control. Template RNA was prepared from the indicated tissues. Data are given as means  $\pm$  SEM (3 mice per genotype, 10-week-old males). hypot., hypothalamus; c. cortex, cerebral cortex, WAT, white adipose tissue; sk. mus., skeletal muscle. (B) Representative Western blot demonstrating the expression of *barr2*-HA in the liver of hep-barr2-OE mice. Please note that the AAV used for generating the hep-barr2-OE mice encoded an HA-tagged version of *barr2*. (C) Glucose production by hepatocytes from hep-barr2-OE mice and control littermates. Glucagon-induced hepatic glucose output is significantly reduced in hepatocytes from hep-barr2-OE mice. Data are given as means  $\pm$  SEM of three independent experiments, each carried out in duplicate. \*\* $p < 0.01$ , as compared to control (Student's t-test).



**Supplemental Figure 12. Hepatic *barr2* expression is down-regulated in mice maintained on a high-fat diet. (A, B)** Hepatic *barr2* (A) and *barr1* (B) transcript levels of WT C57BL/6 mice. Mice were maintained on regular chow (RC) or a high-fat diet (HFD; for 8 weeks). *Barr2* and *barr1* transcript levels were examined via qRT-PCR using  $\beta$ -actin expression as an internal control. Data are given as means  $\pm$  SEM (n=10 mice per group, 16-week-old males). \*\*p<0.01, as compared to RC (Student's t-test).

**Supplemental Table S1. Metabolic Parameters of Hep-Barr2-KO Mice and their Control Littermates**

	Control	Hep-barr2-KO
Body weight (g)	24.2 ± 0.5	24.0 ± 0.3
Liver weight (g)	1.00 ± 0.03	0.94 ± 0.03
Blood glucose (fed, mg/dl)	120 ± 4	141 ± 2**
Blood glucose (fasted, mg/dl )	67.0 ± 3.7	79.5 ± 4.3*
Plasma insulin (fed, ng/ml)	1.40 ± 0.18	1.02 ± 0.16
Plasma insulin (fasted, ng/ml)	0.39 ± 0.05	0.50 ± 0.10
Plasma glucagon (fed, pg/ml)	69.3 ± 5.7	76.3 ± 4.8
Plasma glucagon (fasted, pg/ml)	89.1 ± 7.5	105.1 ± 3.9

Mice (males) maintained on regular chow had free access to food (fed) or were fasted for 12 hr overnight. Data represent means ± SEM (14-20 mice per group for blood glucose measurements; 7-10 mice per group for all other parameters; mouse age: 10-16 weeks).

\*p<0.05, \*\*p<0.01, as compared to the corresponding control value (Student's t-test).

**Supplemental Table S2. Metabolic Parameters of Hep-Barr1-KO Mice and their Control Littermates**

	Control	Hep-barr1-KO
Body weight (g)	28.1 ± 2.0	27.0 ± 1.4
Blood glucose (fed, mg/dl)	129 ± 5	128 ± 5
Blood glucose (fasted, mg/dl)	53.3 ± 3.9	47.4 ± 2.7
Plasma insulin (fed, ng/ml)	1.61 ± 0.17	1.30 ± 0.22
Plasma insulin (fasted, ng/ml)	0.73 ± 0.25	0.57 ± 0.13
Plasma glucagon (fed, pg/ml)	52.3 ± 4.1	57.9 ± 4.2
Plasma glucagon (fasted, pg/ml)	71.6 ± 7.8	67.4 ± 5.1

Mice (males) maintained on regular chow had free access to food (fed) or were fasted for 12 hr overnight. Data represent means ± SEM (7-10 mice per group; mouse age: 12-18 weeks).

**Supplemental Table 3. Metabolic Parameters of Hep-Barr2-OE Mice and their Control Littermates**

	Regular Chow		HFD	
	Control	Hep-barr2-OE	Control	Hep-barr2-OE
Body weight (g)	33.6 ± 1.4	31.9 ± 1.2	50.2 ± 0.5	50.8 ± 1.0
Liver weight (g)	1.40 ± 0.13	1.28 ± 0.05	2.07 ± 0.08	2.41 ± 0.09*
Liver triglyceride (µg per mg protein)	320 ± 23	374 ± 26	871 ± 65	1,184 ± 108*
Liver glycogen (mg per mg protein)	0.050 ± 0.004	0.041 ± 0.004	0.055 ± 0.005	0.057 ± 0.011
Blood glucose (fed, mg/dl)	129 ± 3	115 ± 3*	215 ± 15	173 ± 4*
Blood glucose (fasted, mg/dl)	79.6 ± 4.0	66.7 ± 1.7**	110 ± 5	89.6 ± 5.7*
Plasma insulin (fasted, ng/ml)	0.66 ± 0.13	0.50 ± 0.10	3.43 ± 0.41	4.06 ± 0.84
Plasma glucagon (fasted, pg/ml)	56.6 ± 4.1	63.2 ± 4.4	61.5 ± 5.8	56.3 ± 4.4

Mice (males) were maintained on either regular chow or a high-fat diet (HFD). Mice had free access to food (fed) or were fasted for 12 hr overnight. Data are given as means ± SEM (14-20 mice per group for blood glucose measurements; 7-10 mice per group for all other parameters; mouse age: regular chow mice, ~10-12 weeks; HFD mice, ~20 weeks). \*p<0.05, \*\*p<0.01, as compared to the corresponding control value (Student's t-test).

## Supplemental Methods

### Mouse maintenance and diet

Mice were fed ad libitum and kept on a 12-h light, 12-h dark cycle. Mice were maintained either on a standard mouse chow (4% (w/w) fat content; Zeigler) or a high-fat diet (35.5 % (w/w) fat content; # F3282, Bioserv). All animal experiments were conducted according to the US National Institutes of Health Guidelines for Animal Research and were approved by the NIDDK Institutional Animal Care and Use Committee.

### Generation of mutant mice

To selectively inactivate *barr2* or *barr1* in hepatocytes, we used floxed *barr2* or *barr1* mice in which exon 2 was flanked by loxP sites (*fl/fl barr2* and *fl/fl barr1* mice, respectively). The *fl/fl barr2* mice had a pure C57BL/6 genetic background (1). The *fl/fl barr1* mice were initially obtained on a mixed background (C57BL/6 x 129R1) (Kim, J., Lefkowitz, R.J., et al., manuscript in preparation) and then backcrossed for multiple generations (>7) onto a C57BL/6 background (Taconic). The *fl/fl barr2* mice (8-week-old males) were injected, via the tail vein, with an adeno-associated virus (AAV) coding for Cre recombinase (AAV-TBG-CRE;  $10^{11}$  genomic copies per mouse) (2). This virus directs the selective expression of Cre recombinase in hepatocytes (Cre expression is under the transcriptional control of the hepatocyte-selective thyroxine-binding globulin (TBG) promoter). As a result, injection of floxed *barr2* mice with the AAV-TBG-CRE virus led to the selective inactivation of *barr2* in hepatocytes (hep-*barr2*-KO mice) (Figures S1A and S1B). By using the same strategy, we also generated hep-*barr1*-KO mice (Figures S3A and S3B). For control purposes, we injected floxed *barr2* or *barr1* mice with another virus, AAV-TBG-EGFP (2), that codes for EGFP which is physiologically inert. Both viruses were obtained from the Vector Core of the University of Pennsylvania (Philadelphia, PA). We used a similar strategy to generate mice that selectively overexpressed *barr2* in hepatocytes (hep-*barr2*-OE mice). In this case, wild-type (WT) C57BL/6 mice (8-week-old males; Taconic) were injected with an AAV coding for an HA epitope-tagged version of rat *barr2* under the transcriptional control of

the TBG promoter (source of plasmid: Addgene; source of virus: Vector Core of the University of Pennsylvania).

Mouse phenotyping studies were initiated two weeks after virus administration.

### **Isolation of primary mouse hepatocytes and glucose production assay**

Primary mouse hepatocytes were isolated from livers of mice that were at least 8 weeks old by using a two-step collagenase perfusion protocol (3). Hepatocytes were cultured in collagen I-coated 6-well plates ( $5 \times 10^5$  cells per well) in DMEM containing 10% FBS (GIBCO-BRL). The medium was changed after 4 h with DMEM supplemented with penicillin (100 U/ml) and streptomycin (100  $\mu$ g/ml). To stimulate glucose production, the medium was replaced with glucose- and phenol red-free DMEM supplemented with gluconeogenic substrates (20 mM sodium lactate and 2 mM sodium pyruvate, respectively), followed by an overnight incubation step at 37 °C. Subsequently, hepatocytes were incubated in the same medium in the absence or presence of glucagon (10 and 100 nM) for 4 h at 37 °C. The culture medium was then collected for the measurement of glucose levels using a glucose kit (Sigma).

In a subset of experiments, primary mouse hepatocytes were pre-incubated with or without PTX (300 ng/ml; Tocris) for 2 hr, and then treated with glucagon (10 nM) or isoproterenol (1 and 10  $\mu$ M).

### **Physiological studies**

All in vivo metabolic tests were performed with male mice (age range: 10-20 weeks) using standard procedures. In brief, prior to i.p. glucose tolerance tests (IGTT), mice were fasted overnight for 12 h. Blood glucose concentrations were determined using blood collected from the tail vein immediately before and at defined time points after i.p. injection of glucose (regular chow, 2 g/kg; HFD, 1 g/kg). Glucagon challenge tests (GCT) were carried out using mice that had been fasted for 4 h. Blood glucose levels were determined at various time points after i.p. injection of glucagon (hep-barr2-KO mice, 16  $\mu$ g/kg; hep-barr2-OE mice, 100  $\mu$ g/kg). For pyruvate tolerance tests (PTT), mice were fasted overnight for ~12 h and then injected i.p. with sodium pyruvate (2 g/kg), followed by the monitoring of blood glucose levels. Insulin tolerance tests (ITT) were

carried out with mice that had been fasted for 4 h. Mice were then injected i.p. with human insulin (regular chow, 0.75 U/kg; HFD, 1 U/kg; Novo Nordisk), and changes in blood glucose levels were measured at defined time points. For a subset of studies, mice were injected with an anti-GCGR antibody (10 mg/kg, mAb7.v44; Genentech) (4) 24 h prior to glucose or pyruvate injections. This antibody was a kind gift by Dr. Bernard B. Allan (Genentech Inc., South San Francisco, CA). Blood glucose levels were determined using an automated blood glucose reader (Glucometer Elite Sensor; Bayer). The plasma insulin and glucagon levels shown in the Supplemental Tables were determined by using ELISA (Crystal Chem Inc.) or RIA (Millipore) kits, respectively, following the manufacturers' instructions.

To study glucose-induced changes in plasma insulin, glucagon, and GLP-1 levels (Supplemental Figure 2), mice were fasted overnight for ~12 h and then injected with glucose (2 g/kg i.p.). Blood samples were collected from the tail vein at different time points (0, 5, 15 and 30 min) into EDTA-coated tubes and centrifuged for plasma collection (3,000 g, 5 min, 4 °C). Glucagon and GLP-1 assays were carried out in the presence of proteinase inhibitor aprotinin and DPP-4 inhibitor (Sigma). Plasma insulin, glucagon, and GLP-1 levels were determined by using commercially available ELISA kits (insulin and GLP-1, Crystal Chem Inc.; glucagon, Mercodia).

The anti-GCGR antibody used in this study (mAb7.v44) is a sequence variant of mAb7 first described by Koth et al. (5). The specificity and biological properties of mAb7.v44 are described in detail by Solloway et al. (6), although mAb7.v44 is not specifically identified by name in this study. In fact, all data shown in the figures labeled 'anti-GCGR', including Fig. S1 (6) were generated by using the mAb7.v44 antibody.

### **Measurement of hepatic glycogen and triglyceride levels**

Liver glycogen was measured with a commercially available glycogen assay kit (Sigma,) according to the manufacturer's protocol. Hepatic triglyceride levels were determined by using a published procedure (7).

### **CRE-luciferase reporter assay**

Initially, primary hepatocytes prepared from WT mice (C57BL/6; Taconic) were treated with either *barr2* siRNA (On Target plus siRNA SMARTpools, GE Dharmacon) or scrambled control siRNA (GE Dharmacon) using Lipofectamine RNAiMAX transfection reagent (Thermo Fisher Scientific). About 12 h later, hepatocytes were infected with adenoviruses coding for CRE-luc (CRE, cAMP response element; luc, luciferase) and  $\beta$ -gal (both viruses were a kind gift by Dr. Rebecca Berdeaux, University of Texas Health Science Center, Houston, TX) (10 M.O.I.). About 24 h after virus treatment, hepatocytes ( $3 \times 10^5$  cells per well) were incubated in 12-well plates for 5 h at 37 °C with 10 or 100 nM of glucagon. After this incubation step, luciferase assays were performed as described previously (8).

### **cAMP assay**

Primary mouse hepatocytes were isolated and resuspended in phenol red-free William's medium at a density of  $1 \times 10^6$  cells/ml. Media were supplemented with 500  $\mu$ M IBMX. Subsequently, 5  $\mu$ l aliquots of the cell suspension were added to white-bottom 384-well plates (~5,000 cells per well) and incubated with increasing concentrations of glucagon (added in a 5  $\mu$ l volume) for 25 min at 37 °C. After this incubation step, cells were lysed and glucagon-induced changes in intracellular cAMP levels were determined by using a FRET-based cAMP detection kit, following the manufacturer's protocol (cAMP dynamic 2 kit; Cisbio Bioassays).

In a subset of experiments involving PTX-treated mouse hepatocytes, we used a modified cAMP assay protocol to study cAMP levels in attached cells. Hepatocytes were isolated and cultured in collagen I-coated 6-well plates ( $5 \times 10^5$  cells per well) in culture medium (DMEM with 10% FBS; GIBCO-BRL) supplemented with penicillin (100 U/ml) and streptomycin (100  $\mu$ g/ml). The medium was replaced with the same medium after 4 h. On the second day, cells were washed once with PBS and phenol red-free William's medium supplemented with 500  $\mu$ M IBMX was added. Cells were then stimulated with different ligands for 30 min at 37° C. A subset of cells was pre-incubated with PTX (300 ng/ml) for 2 hr prior to ligand stimulation. After the ligand incubation step, cells were lysed and intracellular cAMP levels were determined by using a FRET-based cAMP

detection kit, following the manufacturer's protocol (cAMP dynamic 2 kit; Cisbio Bioassays).

### **GCGR internalization assay**

The internalization of hepatic GCGRs was monitored via radioligand ( $^{125}\text{I}$ -glucagon) binding as described previously (9). Primary hepatocytes from  $\beta$ -arrestin mutant mice and control littermates were seeded onto collagen-coated 24-well plates ( $1.5 \times 10^5$  cells per well). Cells were cultured overnight and then washed twice with warm binding buffer (DMEM containing 0.1% BSA and 20 mM HEPES, pH 7.4) and incubated at 37 °C for 1 h (starvation step). Hepatocytes were then incubated in the absence or presence of glucagon (100 nM) for 30 min at 37° C. Subsequently, plates were kept on ice and cell surface GCGRs were labeled with 1 nM of  $^{125}\text{I}$ -glucagon per well (2200 Ci/mmol; PerkinElmer). Cells were incubated with the radioligand for 2 h at 4° C in a 200  $\mu\text{l}$  volume. Non-specific binding was determined in the presence of 1  $\mu\text{M}$  glucagon. All binding reactions were carried out in triplicate. Unbound ligand was removed by three washes with ice-cold binding buffer. Cells were then lysed in ice-cold 0.8 M NaOH for 1 h. Subsequently, cell lysates were transferred to glass tubes, and radioactivity was measured using a gamma counter (PerkinElmer).

### **BRET assay**

The ability of the GCGR to recruit both  $\beta$ -arrestins was assessed in transfected COS-7 cells (ATCC, Manassas, VA) using a bioluminescence resonance energy transfer (BRET) assay. A GCGR-*Renilla* luciferase fusion construct (GCGR-Luc) served as the BRET donor (a kind gift by Dr. Eric Xu, Van Andel Research Institute, Grand Rapids, MI). As BRET acceptors, we used plasmids coding for Venus-tagged versions of barr2 (V-barr2) or barr1 (V-barr1), respectively (10). In brief, COS-7 cells were seeded into 100 mm dishes and transfected at 80-90% confluency using Lipofectamine™ 2000 (Invitrogen; 2  $\mu\text{l}$  of Lipofectamine 2000 per 1  $\mu\text{g}$  of DNA). Cells were co-transfected with 0.2  $\mu\text{g}$  of the GCGR-Luc plasmid and 2  $\mu\text{g}$  of V-barr2 (or V-barr1) DNA. BRET measurements were performed as described in detail previously (10, 11). Cells were incubated with increasing concentrations of glucagon (0-10  $\mu\text{M}$ ) for 25 min at 28°C, followed by the addition of 5

$\mu$ M coelenterazine-*h* (luciferase substrate; Nanolight Technology). The resulting BRET data were analyzed using GraphPad Prism 6.04 (GraphPad Software).

### **Hyperinsulinemic euglycemic clamp study**

Clamp studies were performed as described earlier (12). In brief, hep-barr2-KO mice and control littermates (20-week-old males) were catheterized at the left common carotid artery and the right jugular vein. Clamps were performed on unrestrained, conscious mice after 5 h food restriction. The insulin clamp was initiated at  $t=0$  min with a priming bolus (64 mU/kg) of human insulin (Humulin R; Eli Lilly), followed by an infusion (3.6 mU/kg/min) delivered at a pump (CMA Microdialysis) rate of 0.1  $\mu$ l/min from 0 to 120 min. Euglycemia (~120–150 mg/dl) was maintained during clamps by measuring blood glucose every 10 min and infusing 45% dextrose as necessary. The clamp steady state was achieved within 80-120 min.. Glucose infusion rate (GIR) was expressed as mg/kg/min. Plasma insulin levels (human) during the clamp were determined by using an insulin ELISA kit for human insulin (Crystal Chem).

### **Western blotting**

Mouse tissues or hepatocytes were lysed in RIPA buffer (Sigma) containing proteinase and phosphatase inhibitors (Roche). Protein lysates were subjected to SDS-PAGE after denaturation of proteins at 95 °C. Immunoblotting studies were performed using standard procedures. Western blots were scanned and validated with an infrared imaging system (Odyssey CLx; LI-COR Biosciences). All antibodies used for Western blotting were from Cell Signaling: barr2 (Cat# 3857), barr1 (Cat# 4674), p-Akt-S473 (Cat# 9271), p-Akt-T308 (Cat# 2965), total Akt (Cat# 9272), p-GSK3 $\alpha/\beta$  (Cat# 9331), total GSK3 $\alpha/\beta$  (Cat #5676), anti-HA (Cat# 3724), and  $\beta$ -actin (Cat# 3700).

### **RNA extraction and qRT-PCR**

Total mRNA was extracted from hepatocytes or different mouse tissues using the RNeasy Mini Kit (Qiagen), followed by DNase I treatment (Invitrogen). cDNAs were prepared from total mRNA by using a reverse transcriptase kit (SuperScript® III Reverse Transcriptase, Invitrogen). Gene expression levels were measured via qRT-PCR using

QuantiTect primers (Qiagen): QT00495404 (*barr2*), QT00152880 (*barr1*), QT00114625 (*G6Pase*), and QT00153013 (*Pepck*). qRT-PCR studies were carried out as described in detail previously (13). Gene expression data were normalized relative to the expression of  $\beta$ -actin (QT01136772).

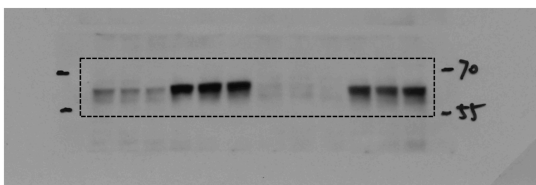
## Supplemental References

1. Urs NM, Gee SM, Pack TF, McCorvy JD, Evron T, Snyder JC, et al. Distinct cortical and striatal actions of a beta-arrestin-biased dopamine D2 receptor ligand reveal unique antipsychotic-like properties. *Proc Natl Acad Sci U S A*. 2016.
2. Miller RA, Chu Q, Le Lay J, Scherer PE, Ahima RS, Kaestner KH, et al. Adiponectin suppresses gluconeogenic gene expression in mouse hepatocytes independent of LKB1-AMPK signaling. *J Clin Invest*. 2011;121(6):2518-28.
3. Neufeld DS. Isolation of rat liver hepatocytes. *Methods Mol Biol*. 1997;75:145-51.
4. Mukund S, Shang Y, Clarke HJ, Madjidi A, Corn JE, Kates L, et al. Inhibitory mechanism of an allosteric antibody targeting the glucagon receptor. *J Biol Chem*. 2013;288(50):36168-78.
5. Koth CM, Murray JM, Mukund S, Madjidi A, Minn A, Clarke HJ, et al. Molecular basis for negative regulation of the glucagon receptor. *Proc Natl Acad Sci U S A*. 2012;109(36):14393-8.
6. Solloway MJ, Madjidi A, Gu C, Eastham-Anderson J, Clarke HJ, Kljavin N, et al. Glucagon Couples Hepatic Amino Acid Catabolism to mTOR-Dependent Regulation of alpha-Cell Mass. *Cell Rep*. 2015;12(3):495-510.
7. Folch J, Lees M, and Sloane Stanley GH. A simple method for the isolation and purification of total lipides from animal tissues. *J Biol Chem*. 1957;226(1):497-509.
8. Conkright MD, Guzman E, Flechner L, Su AI, Hogenesch JB, and Montminy M. Genome-wide analysis of CREB target genes reveals a core promoter requirement for cAMP responsiveness. *Mol Cell*. 2003;11(4):1101-8.
9. Krilov L, Nguyen A, Miyazaki T, Unson CG, Williams R, Lee NH, et al. Dual mode of glucagon receptor internalization: role of PKCalpha, GRKs and beta-arrestins. *Exp Cell Res*. 2011;317(20):2981-94.
10. Gimenez LE, Kook S, Vishnivetskiy SA, Ahmed MR, Gurevich EV, and Gurevich VV. Role of receptor-attached phosphates in binding of visual and non-

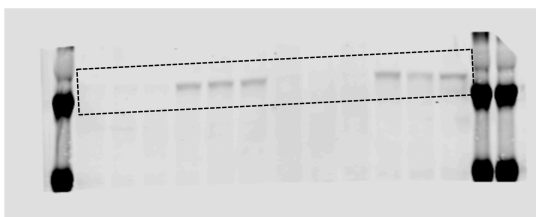
- visual arrestins to G protein-coupled receptors. *J Biol Chem.* 2012;287(12):9028-40.
11. Ruiz de Azua I, Nakajima K, Rossi M, Cui Y, Jou W, Gavrilova O, et al. Spinophilin as a novel regulator of M3 muscarinic receptor-mediated insulin release in vitro and in vivo. *FASEB J.* 2012;26(10):4275-86.
  12. Godlewski G, Jourdan T, Szanda G, Tam J, Cinar R, Harvey-White J, et al. Mice lacking GPR3 receptors display late-onset obese phenotype due to impaired thermogenic function in brown adipose tissue. *Sci Rep.* 2015;5:14953.
  13. Jain S, Ruiz de Azua I, Lu H, White MF, Guettier JM, and Wess J. Chronic activation of a designer G(q)-coupled receptor improves beta cell function. *J Clin Invest.* 2013;123(4):1750-62.

Uncropped gels for Figure 1B

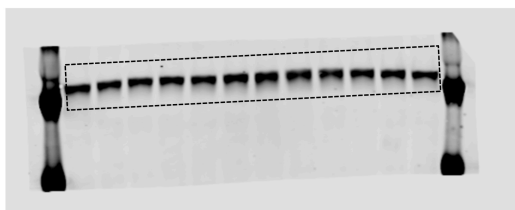
p-Akt  
(T308)



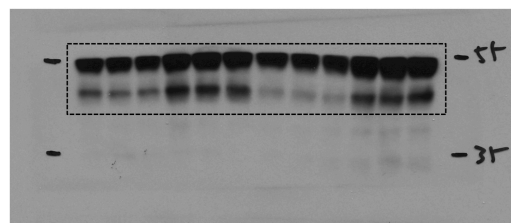
p-Akt  
(S473)



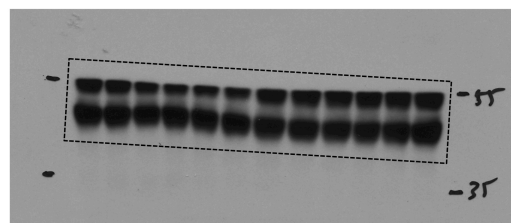
total  
Akt



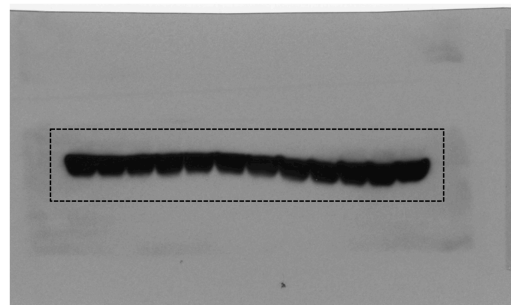
p-GSK3 $\alpha/\beta$



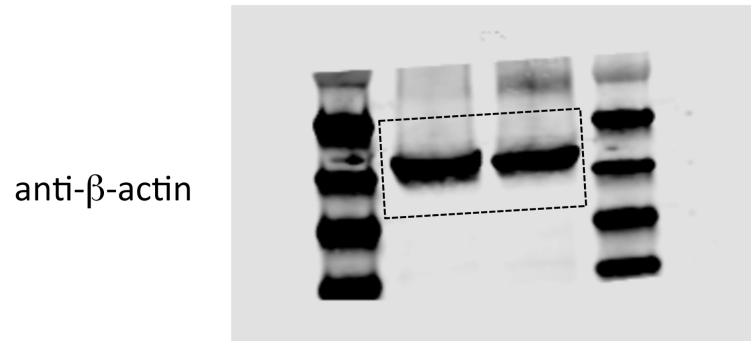
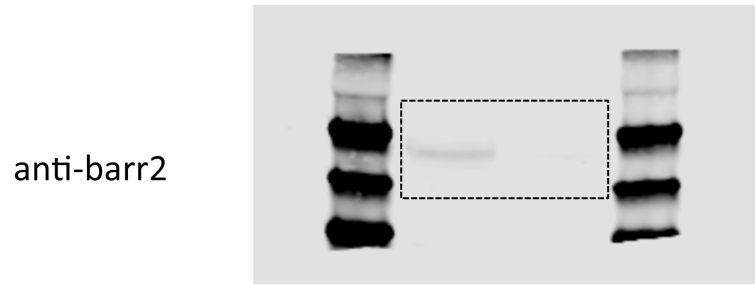
total  
GSK3 $\alpha/\beta$



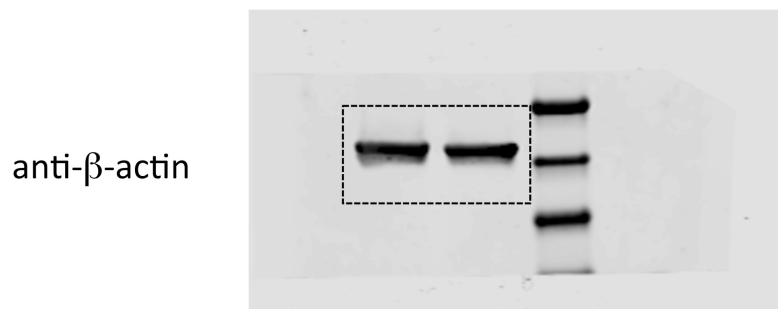
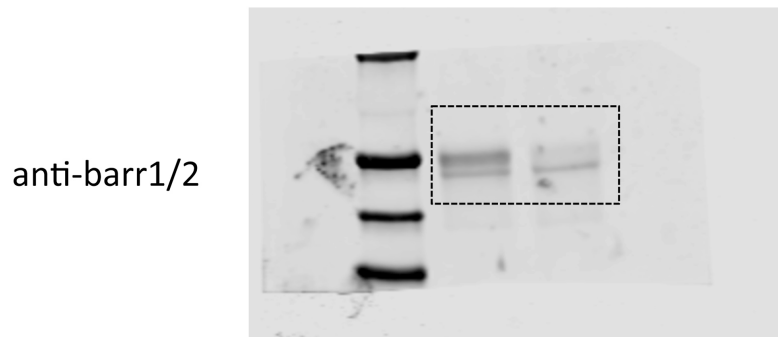
$\beta$ -Actin



Uncropped gels for Supplemental Figure 1B



Uncropped gels for Supplemental Figure 5B



Uncropped gels for Supplemental Figure 11B

